Membrane transport of anandamide through resealed human red blood cell membranes

Inge N. Bojesen[1,*] and Harald S. Hansen[†]

Department of Medical Biochemistry and Genetics,* Laboratory B, University of Copenhagen, The Panum Institute, DK-2200 Copenhagen N, Denmark; and Department of Pharmacology,† Danish University of Pharmaceutical Sciences, DK-2100 Copenhagen Ø, Denmark

Abstract The use of resealed red blood cell membranes (ghosts) allows the study of the transport of a compound in a nonmetabolizing system with a biological membrane. Transmembrane movements of anandamide (*N*-arachidonoylethanolamine, arachidonoylethanolamide) have been studied by exchange efflux experiments at 0°C and pH 7.3 with albumin-free and albumin-filled human red blood cell ghosts. The efflux kinetics is biexponential and is analyzed in terms of compartment models. The distribution of anandamide on the membrane inner to outer leaflet pools is determined to be 0.275 ± 0.023, and the rate constant of unidirectional flux from inside to outside is 0.361 ± 0.023 s^{-1}. The rate constant of unidirectional flux from the membrane to BSA in the medium ($[BSA]_o$) increases with the square root of $[BSA]_o$ in accordance with the theory of an unstirred layer around ghosts. Anandamide passed through the red blood cell membrane very rapidly, within seconds. At a molar ratio of anandamide to BSA of <1, membrane binding of anandamide increases with increasing temperatures between 0°C and 37°C, and the equilibrium dissociation constants are in the nanomolar range. The nature of membrane binding and the mechanism of membrane translocation are discussed.— Bojesen, I. N., and H. S. Hansen. **Membrane transport of anandamide through resealed human red blood cell membranes. *J. Lipid Res.* 2005.** 46: **1652–1659.**

Supplementary key words transmembrane movement • erythrocyte ghosts • membrane binding • exchange efflux

Anandamide (*N*-arachidonoylethanolamine, arachidonoylethanolamide) is a member of the lipid molecule group called the *N*-acylethanolamines (1, 2), and it is also an agonist for the cannabinoid receptors (3–5), for the vanilloid receptor (6, 7), and for the regulation of the exchange efflux kinetics-1 potassium channel (8). Other anandamide receptors also may exist (9). The synthesis of anandamide from a precursor phospholipid is catalyzed by a specific phospholipase D (10–12) that may be intracellularly located in membranes (10). To affect other cells, anandamide has to pass through the plasma membrane of the cell where it is generated. Furthermore, extracellular anandamide has to pass through a plasma membrane to be hydrolyzed by the fatty acid amide hydrolase (10, 13) that is found in intracellular membranes (14, 15). Anandamide has important mediator roles in inflammation (16), in pain modulation (17), and in the vascular system (18). In the extracellular compartment, anandamide binds to serum albumin (19, 20).

Cellular uptake of anandamide in the monomeric form occurs as a sequence of at least three steps: release from its binding protein, membrane translocation, and binding by intracellular binding proteins and/or metabolic transformation by intracellular enzymes. Several cell types have been used to study the cellular uptake (15, 21, 22). In spite of much effort, it is still unsettled whether the membrane translocation is governed by a simple diffusion through the lipid bilayer of the membrane, whether proteins are involved, or whether both mechanisms exist simultaneously (23–27). A similar discussion of the transport mechanism, for and against a simple diffusion through the lipid bilayer, has been going on for years with regard to fatty acids. However, in contrast to anandamide, these lipophilic molecules are present in aqueous phases as ions. Normally, ions need transport proteins to pass biological membranes. Several proteins have been isolated that are claimed to be responsible for the transmembrane movement of fatty acids, although it is not explicitly stated whether the membrane proteins facilitate the transport of the ionized or the unionized molecules (28–30). The opinion of others is that transport across cellular membranes occurs by diffusion through the lipid bilayer of the neutral form of fatty acids (31, 32). Finally, both mechanisms may exist, but again, no clear solution to the problem has emerged.

We have used the erythrocyte membrane that classically has been used for transport studies. Resealed red blood cell membranes (ghosts) can be used as a model system

Manuscript received 17 December 2004 and in revised form 31 March 2005 and in re-revised form 17 May 2005.

Published, JLR Papers in Press, June 1, 2005.
DOI 10.1194/jlr.M400498-JLR200

[1] To whom correspondence should be addressed.
e-mail: norby@imbg.ku.dk

for cellular plasma membranes in general, in which interference from cytosolic proteins and metabolizing enzymes is avoided. The limitation of the model is that membrane lipid composition, cytoskeleton proteins, and transmembrane proteins are to a certain extent different from those of other cell types.

Our conclusion regarding fatty acid uptake through human red blood cell membranes is that proteins are important, but as determinants of specific lipid domains through which the fatty acids in neutral form are transported by diffusion (33–35). Kleinfeld, Storms, and Watts (32) have also reported that fatty acid transport across red blood cell ghosts is reasonably well described by transport across the lipid phase of the membrane. The aim of the present study is to determine the rate by which anandamide passes through a biological membrane and in this way learn about the transport mechanism. Our results show an extremely rapid transport of anandamide through the erythrocyte membrane (within seconds), but they do not give an unambiguous elucidation of the transport mechanism.

MATERIALS AND METHODS

Materials

Radioactive anandamide ([*N*-arachidonoyl-5,6,8,9,11,12,14,15-^{3}H]ethanolamine; specific activity = 215 Ci mmol^{-1}) was obtained from Perkin-Elmer Life Sciences, Inc. (Boston, MA), and unlabeled anandamide was purchased from Biomol Research Laboratories, Inc. The purity of both anandamide preparations was controlled by chromatography on a Sephadex LH-20 column (160 × 0.8 mm) using dichloromethane as eluent. [^{3}H]inulin (specific activity = 5 Ci mmol^{-1}) was from Amersham Biosciences (Hillerød, Denmark). The scintillation fluid Ultima Gold was from Packard Instrument Co., Inc., and BSA fraction V (fatty acid-free) was from Boehringer Mannheim GmbH.

Preparation of erythrocyte ghosts

The preparation of a uniform population of BSA-free and BSA-filled resealed "pink" ghosts from freshly drawn human blood was carried out as described previously (36). The resealed ghosts were isolated from the hemolysate by centrifugation and washed at 0°C with 165 mM KCl, 2 mM phosphate buffer, pH 7.3, containing 0.02 mM EDTA/EGTA (1:1, v/v) (buffer I). They were stored in the same buffer containing BSA of appropriate concentrations and used for experiments within 2 days. The density of ghosts is 1.02 g/ml, and for calculations, we assumed 1 g of packed ghosts = 1 ml. Eight donors, including both men and women (age 21–64 years), were used.

Preparation of incubation buffers

[^{3}H]anandamide and unlabeled anandamide were dissolved in 50 μl of benzene, just enough to moisten 200 mg small glass beads (diameter of 0.1 mm). The benzene was sublimated at low pressure, and incubation buffers were prepared by shaking the anandamide-loaded beads with a solution of BSA in buffer I for 15 min at room temperature.

Membrane binding experiments

BSA-free ghosts were packed by centrifugation for 7 min at 30,000 *g* at 4°C in a Sorval RC 5C plus. Packed ghosts were incubated with incubation buffer at a ratio of 2:3 for 50 min at 0°C. After centrifugation, aliquots of the incubation buffer were taken for scintillation counting, and the rest was removed. The ghosts were washed in buffer I without BSA, and after removal of the supernatant duplicate samples of ghosts (~25 mg), they were taken for weighing and counting.

The extracellular volume in the initial packed ghosts (20%) was measured with [^{3}H]inulin in experiments carried out parallel with the binding experiments. The extracellular volume after washing was 10%. The uptake (M) of anandamide by ghost membranes was calculated on the basis of the concentration in incubation buffer before (C_b; dpm/ml) and after (C_a; dpm/ml) the incubation as:

$$M = (C_b\ 1.5 - C_a\ (1.5 + 0.20))/0.80\ Sp\ nmol/g \qquad (Eq.\ 1)$$

or directly from dpm in ghosts:

$$M = d \times 1{,}000/(V \times 0.9 \times Sp)\ nmol/g \qquad (Eq.\ 2)$$

where Sp (dpm/nmol) is the specific activity of anandamide and d (dpm/mg) is the radioactivity in V (mg) ghosts. The corresponding molar ratio (ν) of anandamide to BSA is calculated as

$$\nu = C_a/(Sp \times [BSA]) \qquad (Eq.\ 3)$$

The equilibrium constant for the dissociation of anandamide from ghost membranes is defined as

$$K_{dm} = [A]\ (M_{max} - M)/M \qquad (Eq.\ 4)$$

where [A] is the free water phase concentration of anandamide and M_{max} is the maximal binding capacity. The equation can be arranged as:

$$M = M_{max}\ [A]/(K_{dm} + [A]) \qquad (Eq.\ 5)$$

This equation is used to analyze the data by nonlinear regression to determine M_{max} and K_{dm}.

Efflux experiments with ghosts

One volume of packed ghosts was equilibrated with 1.5 volume of incubation buffer at 0°C for 50 min. Radioactive ghosts (with or without interior BSA) were then separated by centrifugation for 7 min at 30,000 *g* from buffer I containing labeled as well as unlabeled anandamide and washed with 10 volumes of buffer I, pH 7.3, at 0°C. These washed suspensions of radioactive ghosts were distributed into 80 mm plastic tubes (inner diameter of 3 mm) and packed by centrifugation for 10 min at 17,000 *g* at 0°C. The supernatant was removed by cutting the plastic tube just below the interface, and the packed radioactive ghosts (~100–200 mg) were injected into 35 ml of vigorously stirred isotope-free buffer I containing BSA and unlabeled anandamide corresponding to the cellular ν value. Serial sampling of cell-free extracellular medium was done with the Millipore-Swinnex filtration technique. Ten to 15 samples were taken at appropriate intervals for the determination of the extracellular accumulation of radioactivity as a function of time. The activity of filtrates was measured by counting 400 μl in 3.9 ml of Ultima Gold. The efflux experiments were all carried out at 0°C, because the rapid efflux of anandamide from ghosts and our manual sampling technique do not allow higher temperature.

In control efflux experiments at low ν (0.065) as well as at higher ν (0.4) with no albumin in the outer medium, we found <3.2% of the radioactivity in the medium. Furthermore, no time-dependent increase in supernatant radioactivity was seen.

THEORY OF EFFLUX

Efflux from BSA-free ghosts

The efflux of labeled anandamide from ghosts to the same concentration of nonlabeled anandamide in the BSA-

containing buffer is an exchange efflux without a concentration gradient. **Figure 1** shows the compartment models we used to account for the efflux kinetics of [^{3}H]anandamide from the ghosts. The mathematics of the corresponding equations and expressions are presented in the Appendix. The exchange kinetics follows a biexponential time course, and the solution of the second-order differential equation that describes the kinetics is (37, 38)

$$1 - a/a_\infty = C1\, e^{-\alpha t} + C2\, e^{-\beta t};\ (C1 + C2) = 1 \quad \textit{(Eq. 6)}$$

The connections between the parameters of the model [B/E, k_m, and k_3 (Fig. 1)] are as follows:

$$k_m = \alpha + \beta - \alpha\beta/(\alpha\, C1 + \beta\, C2) \quad \textit{(Eq. 7)}$$

$$k_3 = \alpha\, \beta/k_m \quad \textit{(Eq. 8)}$$

$$1 + B/E = k_m/(\alpha\, C1 + \beta\, C2) \quad \textit{(Eq. 9)}$$

The efflux data are fitted to obtain a maximum correlation coefficient (R) by nonlinear regression analyses using the software Origin 6. Model parameters are calculated according to equations 7–9.

Efflux from BSA-filled ghosts

A model accounting for anandamide efflux from BSA-filled ghosts to BSA in the medium requires yet another compartment, namely, the intracellular pool of BSA-bound anandamide. However, the reliability of results obtained by fitting to three exponential functions is poor and thus of limited validity. Therefore, we have defined two new constants: k_i for the unidirectional anandamide flow from internal anandamide-BSA complexes to the outer surface of the ghost membrane; and k_m* for the unidirectional flow from the membrane outer surface to BSA in the medium (see model II). The theory of efflux from BSA-filled ghosts is exactly as for BSA-free ghosts and the equations are the same, but the rate constants k_3 and k_m are replaced by k_i and k_m*.

Thus, the exchange kinetics follows a biexponential time course, and the solution of the second-order differential equation describing the kinetics is in this case

$$1 - a/a_\infty = C3\, e^{-\gamma t} + C4\, e^{-\delta t} \quad \textit{(Eq. 10)}$$

and the connection between the parameters of the model is now as follows:

$$k_m^* = \gamma + \delta - \gamma\, \delta/(\gamma\, C3 + \delta\, C4) \quad \textit{(Eq. 11)}$$

$$k_i = \gamma\, \delta/k_m^* \quad \textit{(Eq. 12)}$$

$$1 + Ai/E = k_m^*/(\gamma\, C3 + \delta\, C4) \quad \textit{(Eq. 13)}$$

For parameters, see Fig. 1.

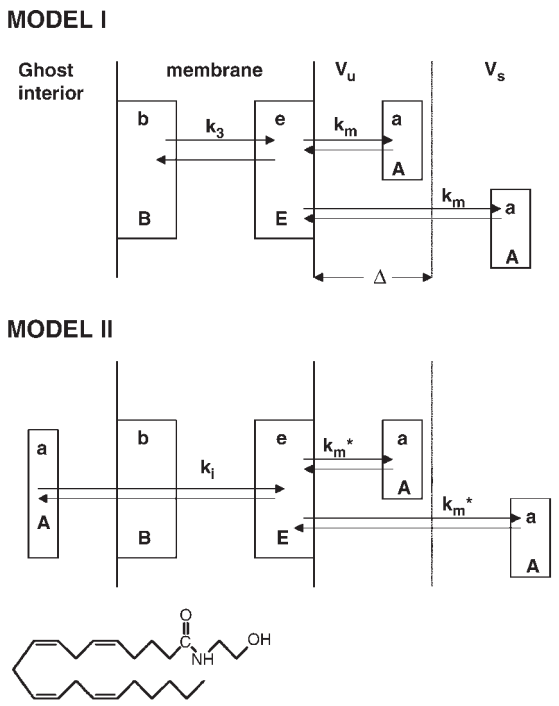

Fig. 1. The compartment models used to account for the efflux of [^{3}H]anandamide from ghosts in nonisotopic equilibrium with the medium. Model I: ghosts without internal serum albumin; model II: ghosts with internal serum albumin. Arrows indicate unidirectional anandamide fluxes. k_3, k_m, k_i, and k_m* are first-order rate constants of fluxes between adjacent compartments. Lowercase letters a, b, and e refer to [^{3}H]anandamide concentrations, and uppercase letters A, B, and E refer to anandamide concentrations. V_u is the unstirred volume around ghosts with the depth Δ, and V_s is the stirred volume around ghosts. At bottom, the chemical formula of anandamide is given.

Scintillation counting

We used a Tri-Carb 2200CA liquid scintillation analyzer from Packard. The efficiency was 67% for ^{3}H in unquenched samples using 3.9 ml of Ultima Gold scintillation fluid. Counting rates were determined to a probable error of <1%.

Statistics and data analyses

The linear and nonlinear regression procedures given by Origin 6 (Microsoft) were used to determine the best fit of the data to the exponentials of the model. The formula to calculate the variations of terms was the general formula

$$\text{var}(T(a,b,c\ldots.)) = \text{var a}\ (dT/da)^2 + \text{var b}\ (dT/db)^2 + \text{var c}\ (dT/dc)^2 + \ldots\ldots\ldots \text{and SD (T) as (var (T)}^{1/2}) \quad \textit{(Eq. 14)}$$

RESULTS

Membrane binding

The equilibrium binding of anandamide monomer to ghosts (without internal BSA) has been determined at 0, 10, 23, and 37°C for a molar ratio (ν) of anandamide to BSA of <1. According to the definition of the equilibrium dissociation constant (K_d), the concentration of anandamide monomer in the water phase is [A] = Kd $\nu/(1 - \nu)$ (19). **Figure 2A**, **B** shows examples of the relationship between the binding (M) and [A] for $\nu < 1$. The maximal binding capacity (M_{max}) was found to be temperature-dependent (**Table 1**). Efflux experiments have mostly been carried out at $\nu = 0.2$, so M has been determined at this ν value and at 0°C. The mean value of M is 5.25 ± 0.39 nmol/g ghosts (n = 9), and ν is 0.198 ± 0.018. To investi-

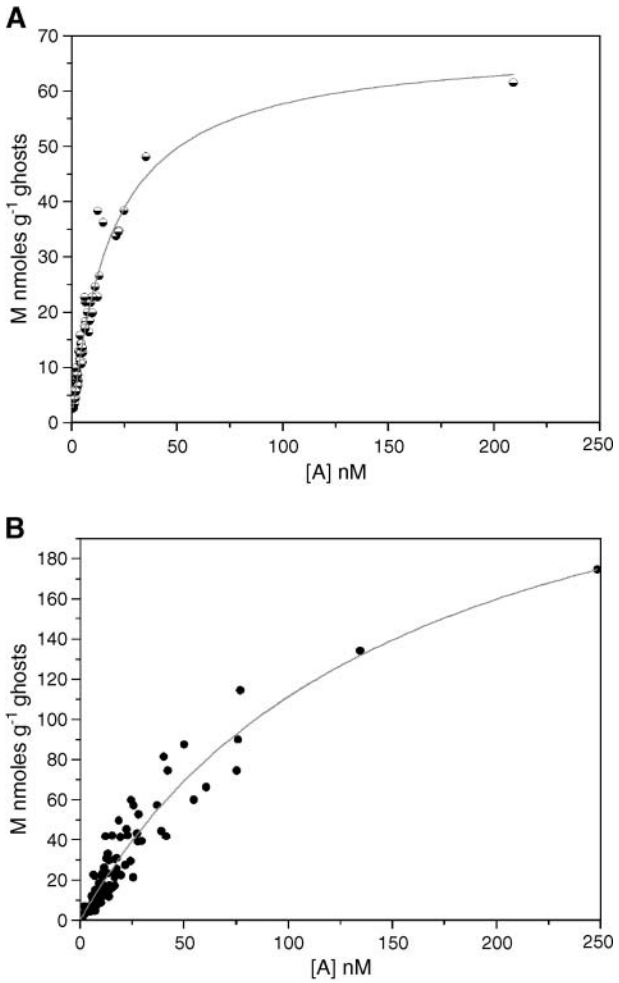

Fig. 2. Data of anandamide binding (M) to BSA-free ghosts at 0°C (A) and at 37°C (B) and corresponding water-phase concentrations represented by $K_d\ \nu/(1-\nu)$ (see text) for ν values <1.

gate whether k_m is dependent on ν, we carried out some of the efflux experiments at other ν values and determined the corresponding membrane binding. For ν = 0.102, M = 2.53 nmol/g, and for ν = 0.784, M = 38.34 nmol/g.

Exchange efflux of anandamide from BSA-free ghosts

The high reproducibility of these experiments enabled us to pool the data of several subsequent injections from the same ghost preparation as well as data from other ghost preparations. We have studied anandamide efflux for $[BSA]_o$ between 7.5 and 60 μM. The data of a series with $[BSA]_o$ = 30 μM is presented semilogarithmically in **Fig. 3**. The curve is not linear, which means that the efflux kinetics of anandamide cannot be described by a closed two-compartment model normally valid for water-soluble compounds. On the other hand, all experiments are well described by the three-compartment closed system and by the three-compartment approximation shown in Fig. 1. The rate of efflux is extremely rapid, and at 0°C, when $[BSA]_o$ is 30 μM, ~90% equilibrium is obtained within 5 s The model parameters are analyzed according to equations 7–9 and shown in **Table 2**. **Figure 4** shows the efflux kinetics from BSA-free ghosts to three different $[BSA]_o$ levels. With a 60 μM $[BSA]_o$, 90% of the labeled anandamide is found in the external medium in <4 s, so with the present technique, no higher concentration of $[BSA]_o$ could be used without severely affecting the reliability of the results. Correspondingly, with $[BSA]_o$ < 7.5 μM, the filters adsorb a tiny amount of albumin and the points are less reliable.

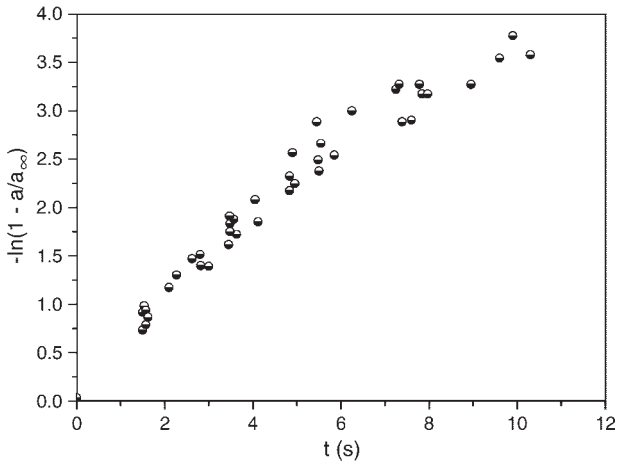

Fig. 3. Exchange efflux kinetics of [^{3}H]anandamide from BSA-free ghosts at 0°C (pH 7.3), ν = 0.2, into the extracellular buffer containing 30 μM BSA and nonlabeled anandamide. a/a_∞ is the ratio of time-dependent [^{3}H]anandamide in the buffer to [^{3}H]anandamide at infinite time.

The most important finding of the analyses is that the two parameters B/E and k_3 are independent of $[BSA]_o$, whereas there is a direct correlation between the rate constant of unidirectional flow from the outer membrane sites to BSA in the medium (k_m) and $[BSA]_o$ (Table 2). The latter effect is understood by the tracer uptake by BSA in an unstirred volume (V_u) and in a stirred volume (V_s) (37, 38). The variable k_m is not dependent on the ν

TABLE 1. M_{max} of ghost membranes for anandamide and K_{dm} of anandamide dissociation from ghost membranes at four different temperatures

Variable	0°C	10°C	23°C	37°C
M_{max} (nmol/g ghosts)	68.35 ± 2.15	70.26 ± 6.38	123.09 ± 2.13	283.11 ± 23.98
K_{dm} (nM)	19.88 ± 1.10	11.21 ± 2.50	37.44 ± 4.49	154.33 ± 18.69
n	63	26	58	96

K_{dm}, equilibrium dissociation constant; M_{max}, maximal binding capacity. n is the number of determinations. One gram of ghosts = 9×10^9 ghosts.

TABLE 2. Model I parameters determined by efflux kinetics using BSA-free resealed red blood cell membranes (ghosts)

$[BSA]_o$	k_3	k_m	B/E	*R*
μM		s^{-1}		
7.5	0.271 ± 0.099	0.482 ± 0,166	0.361 ± 0.208	0.979
7.5	0.337 ± 0.085	0.430 ± 0.120	0.315 ± 0.174	0.983
7.5	0.251 ± 0.067	0.530 ± 0.081	0.293 ± 0.087	0.989
7.5	0.325 ± 0.083	0.453 ± 0.117	0.302 ± 0.116	0.992
Weighted mean		0.487 ± 0.055		
15	0.484 ± 0.142	0.557 ± 0.200	0.261 ± 0.128	0.971
15	0.343 ± 0.065	0.622 ± 0.089	0.297 ± 0.074	0.986
15	0.468 ± 0.103	0.573 ± 0.135	0.201 ± 0.068	0.993
15	0.429 ± 0.088	0.557 ± 0.119	0.262 ± 0.081	0.972
15	0.369 ± 0.059	0.649 ± 0,074	0.255 ± 0.051	0.991
Weighted mean		0.613 ± 0.047		
30	0.188 ± 0.083	1.120 ± 0.368	0.547 ± 0.235	0.988
30	0.494 ± 0.113	0.703 ± 0.139	0.135 ± 0.043	0.994
30	0.361 ± 0.048	0.815 ± 0.062	0.328 ± 0.050	0.994
30	0.171 ± 0.041	1.162 ± 0.204	0.507 ± 0.117	0.996
30	0.409 ± 0.034	0.900 ± 0.038	0.272 ± 0.024	0.992
30	0.444 ± 0.072	0.712 ± 0.093	0.242 ± 0.053	0.993
Weighted mean		0.874 ± 0.013		
		(0.830 ± 0.030)		
60	0.423 ± 0.158	1.076 ± 0.326	0.293 ± 0.125	0.998
60	0.479 ± 0.288	1.118 ± 0.597	0.255 ± 0.205	0.997
60	0.418 ± 0.026	1.120 ± 0.027	0.293 ± 0.017	0.994
Weighted mean	0.361 ± 0.023	1.120 ± 0.011	0.275 ± 0.023	
	(0.391 ± 0.019)		(0.272 ± 0.013)	

The model parameters were calculated according to equations 7–9. B/E is the ratio of anandamide associated with the membrane inner leaflet to anandamide associated with the membrane outer leaflet. For k_3 and k_m, see Fig. 1. *R* is the correlation coefficient. Values in parentheses are weighted means without the two outstanding experiments 1 and 4 for $[BSA]_o$ = 30 μM.

value. Direct experimental verification of this independence was obtained by efflux experiments at low and high ν values. With $[BSA]_o$ = 15 μM, we get k_m = 0.649 ± 0.074 s^{-1} at a low ν value (0.06) and 0.622 ± 0.066 s^{-1} at a high ν value (0.4). When $[BSA]_o$ = 30 μM, we find k_m = 0.712 ± 0.093 s^{-1} at a low ν value (0.05) and 0.815 ± 0.062 s^{-1} at a high ν value (0.4).

Exchange efflux of anandamide from BSA-filled ghosts

We have studied the [^{3}H]anandamide effluxes from BSA-filled ghosts in several series with a minimum of 15 points in each series. Here, the exchange kinetics also follows a biexponential time course (model II; Fig. 1). We have varied $[BSA]_i$ as well as $[BSA]_o$ and kept the ν value between 0.1 and 0.3. **Figure 5** shows exchange efflux kinetics from

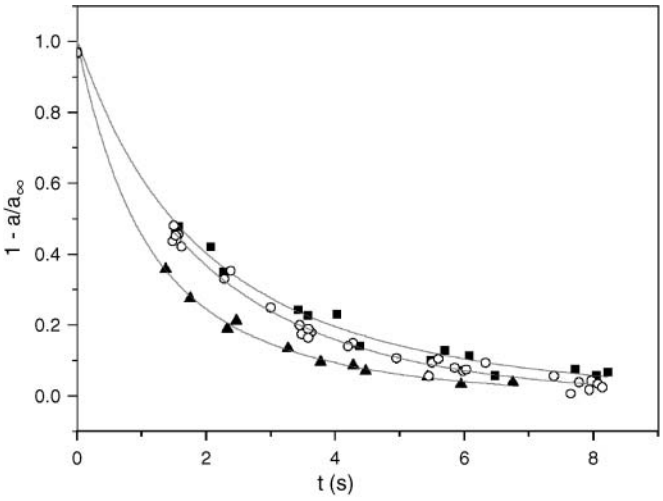

Fig. 4. Rate of [^{3}H]anandamide efflux from BSA-free ghosts at 0°C (pH 7.3), ν = 0.2. For a and a_∞, see legend to Fig. 3. Closed squares, 15 μM $[BSA]_o$; open circles, 30 μM $[BSA]_o$; closed triangles, 60 μM $[BSA]_o$. Solid curves show the nonlinear regression fitting the data to a sum of two exponential terms with known distribution.

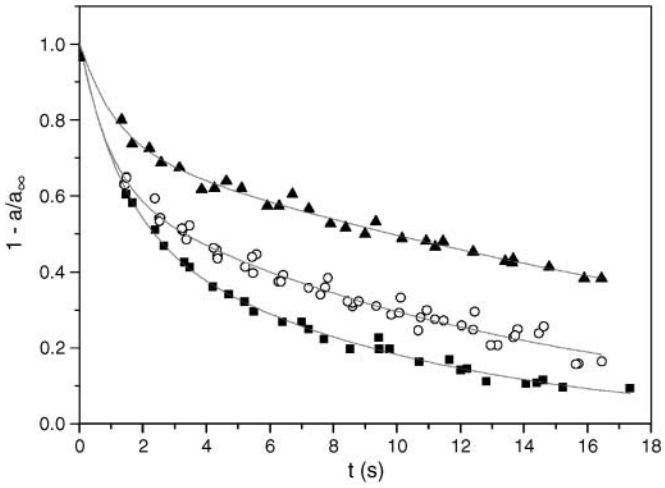

Fig. 5. Rate of [^{3}H]anandamide efflux from BSA-filled ghosts at 0°C (pH 7.3), ν = 0.2. For a and a_∞, see legend to Fig. 3. $[BSA]_o$ is in all three cases 30 μM. Closed squares, 15 μM $[BSA]_i$; open circles, 30 μM $[BSA]_i$; closed triangles, 60 μM $[BSA]_i$. Solid curves show the nonlinear fitting of the data to a sum of two exponential terms with known distribution.

three preparations of ghosts filled with 15, 30, and 60 μM BSA and in all cases injected into a medium containing 30 μM BSA. The lines are nonlinear regression lines fitting the data to a sum of two exponential terms with a known distribution. The efflux rate from BSA-filled ghosts is slower than from BSA-free ghosts but is still rather rapid. The efflux rate—that is, the anandamide release from intracellular anandamide-BSA complexes (30 μM $[BSA]_i$), the transport through the membrane, release from the membrane, and transfer to medium BSA (30 μM $[BSA]_o$)—reaches 80% equilibrium within 16 s (compared with ~4 s for the BSA-free ghost). Changing the $[BSA]_i$ to 60 μM results in 50% equilibrium in ~10 s. The rate constant of anandamide transfer from intracellular BSA complexes to the membrane outer leaflet (k_i) turns out to be strongly dependent on $[BSA]_i$ but not on $[BSA]_o$, whereas k_m* depends only on $[BSA]_o$ and not on $[BSA]_i$ (**Table 3**).

A distinct pattern is seen with regard to the two rate constants k_m* and k_i. Except for the highest $[BSA]_o$, the k_m* values are not much different from k_m determined in experiments with BSA-free ghosts (Table 2), whereas k_i decreases strongly with increasing $[BSA]_i$ no matter which $[BSA]_o$ is used (Table 3). This constant, k_i, was compared with the rate coefficient (δ) of the efflux kinetics determined previously (37, 38). Here, a similar decrease was observed, and again, unstirred volume inside the ghosts can explain this phenomenon.

DISCUSSION

Membrane binding

Both arachidonic acid (33) and anandamide show saturable binding to red blood cell membranes (Fig. 2). The maximal equilibrium binding (M_{max}) of arachidonic acid to red blood cell membranes is 6 nmol/g ghost and is independent of temperature (0–37°C) (33). This independence is interpreted as a binding of the fatty acid anion to membrane protein(s) followed by an instantaneous equilibration between ionized and unionized arachidonic acid and a subsequent diffusion of the neutralized form of arachidonic acid through protein-defined lipid domains. However, in the present study, we found that M_{max} for anandamide was temperature-dependent and much larger than M_{max} for arachidonic acid. This difference may be explained by the primary binding (capture) in the membrane of a neutral molecule and an anion, respectively.

The findings of *a*) an increasing M_{max} with increasing temperatures and *b*) K_{dm} values (Table 1) that are not much different from the K_d values for anandamide dissociation from BSA suggest two mutually contradictory interpretations. *a*) The existence at all temperatures of cholesterol/sphingolipid-rich, liquid-ordered domains in the cell membranes is well known (39). Such domains containing predominantly saturated lipid hydrocarbon chains coexist with more disordered regions occupied by unsaturated phospholipids. One could speculate that the unsaturated anandamide binds to these regions of unsaturated phospholipids and that the disorder of the regions probably would be greater at higher temperature, leaving more space for anandamide. Consequently, the conclusion is that anandamide probably is bound in the lipid phase and not to proteins. *b*) K_{dm} values in the nanomolar range (Table 1) suggest a specific and strong binding to the erythrocyte membrane analogous to the strong binding found for anandamide to BSA (19). In this connection, it is interesting that anandamide is involved in the regulation of certain potassium channels (8). Thus, it is still uncertain how anandamide is bound in the cellular membrane. However, when first bound, the membrane permeation of anandamide and of arachidonic acid in a neutral form may be similar.

Exchange efflux from BSA-free ghosts

Strong evidence for the reliability of the transport model (Fig. 1) is that k_m is directly proportional to the reciprocal value of the square root of $[BSA]_o$, in accordance with the predicted effect of the unstirred layer as described in previous publications (37, 38).

According to the present study, anandamide membrane

TABLE 3. Effects of $[BSA]_i$ and $[BSA]_o$ on the two rate constant k_m* and k_i

$[BSA]_i$	$[BSA]_o$	k_m*	k_m	k_i
	μM		s^{-1}	
Variable	7.5	0.490 ± 0.089 (n = 6)	—	—
0	7.5	—	0.487 ± 0.055 (n = 4)	—
7.5	Variable	—	—	0.188 ± 0.024 (n = 9)
Variable	15	0.612 ± 0.049 (n = 10)	—	—
0	15	—	0.613 ± 0.047 (n = 5)	—
15	Variable	—	—	0.117 ± 0.018 (n = 7)
Variable	30	0.768 ± 0.051 (n = 8)	—	—
0	30	—	0.874 ± 0.01 (n = 7)	—
30	Variable	—	—	0.072 ± 0.008 (n = 6)
Variable	60	0.699 ± 0.074 (n = 2)	—	—
0	60	—	1.120 ± 0.011 (n = 3)	—
60	Variable	—	—	0.043 ± 0.006 (n = 2)

k_m* is the rate constant of anandamide transport from the outer surface of the ghost membrane to medium BSA, and k_i is the rate constant of unidirectional flow from anandamide-BSA complexes inside the ghost to the outer surface of the ghost membrane (see model II in Fig. 1). n is the number of series, with 15–34 points in each series. The rate constants k_m* and k_i are calculated according to equations 11 and 12, respectively.

translocation is extremely rapid. With 60 μM binding protein inside as well as outside the cells, the half-life for translocation through the membrane at 0°C to the extracellular binding protein is ~16 s, so at 37°C, it is probably <1 s. Therefore, data obtained from anandamide uptake studies with lipid membranes lasting for minutes are probably not valid for the measurement of pure translocation processes (27). Furthermore, anandamide uptake studies with micromolar concentrations without albumin in the cell culture media may give false results because of the aggregation and adsorption phenomena. In our experiments, no anandamide is released from the ghosts without albumin in the medium as a result of the very low free water concentration of anandamide (19). This means that anandamide in such experiments is offered to the cells in concentrations that exceed the monomer water-phase concentration by a factor of $>10^3$. Anandamide is a hydrophobic compound, and aggregations occur together with adherence to glass tubes and plastic wells if not bound to albumin (24, 40), so added to buffer directly or dissolved in alcohol, the actual concentration is unknown.

Exchange efflux from BSA-filled ghosts

The exchange efflux from BSA-filled ghosts follows a biexponential time course. The rate constants k_i and k_m* can be determined by equations 11 and 12. The k_m* values are not different from the values of k_m except for one determination from two series at 60 μM (Table 3). The fact that there is only a difference at 60 μM means that the unidirectional flow of anandamide from the intracellular BSA-anandamide complexes to the outer membrane sites can be accounted for by k_i. Because $k_3 >> k_i$, the transport from the small inner membrane pool of anandamide to the outer membrane pool is rapid and release from BSA_i to the inner membrane pool becomes rate-limiting. If anandamide can diffuse quickly through the lipid membrane of erythrocytes, then it should probably also be able to diffuse through the plasma membrane of other cells. This conclusion does not exclude the possibility that anandamide can bind to a pool of intracellular proteins, including fatty acid amide hydrolase, fatty acid binding proteins (41), and/or ceramide binding protein (42).

All of these experiments were performed under steady-state conditions [i.e., the net flux of radioactive anandamide is balanced by an equal and opposite movement of nonradioactive anandamide (exchange efflux)]. This means that they are also valid as uptake experiments. Glaser et al. (27) performed short-term uptake studies of anandamide complexed to BSA, and they favor an uptake mechanism involving diffusion through the lipid bilayer.

In conclusion, our data show that anandamide is able to pass a biological membrane very rapidly, within seconds. Furthermore, this transmembrane movement occurs without ATP consumption and is independent of a concentration gradient or the metabolism of anandamide. However, the mechanism of membrane translocation of anandamide, whether it is a passive diffusion through the lipid bilayer or a protein-facilitated transfer, cannot be unambiguously settled from the present results. As anandamide is an uncharged lipophilic molecule, there may be no energy restriction to keep it on one side of the lipid bilayer and therefore no reason to believe that a protein has to be involved in the transport mechanism.

APPENDIX

In exchange flux, the net flux of labeled anandamide between two subsequent compartments is the product of the unidirectional flux of anandamide and the difference in specific activities. Therefore, the system kinetics can be described by the following first-order linear differential equations, expressed in the first-order rate constants k_3 and k_m (Fig. 1)

$$-db/dt = k_3\, B\, (b/B - e/E) \qquad \textit{(Eq. A1)}$$

$$da/dt = k_m\, E\, (e/E - a/A) \qquad \textit{(Eq. A2)}$$

The total amount of labeled anandamide (T) is the sum of b, e, and a.

$$T = b + e + a \qquad \textit{(Eq. A3)}$$

Because the volume of extracellular medium is >200-fold greater than the ghost volume, we can write

$$A >> (B + E) \text{ and } B/A << 1 \text{ and } E/A << 1 \qquad \textit{(Eq. A4)}$$

By the rearrangement of equation A2 and $E/A << 1$, we get

$$e = (1/k_m)\, da/dt + E/A\, a = (1/k_m)\, da/dt \qquad \textit{(Eq. A5)}$$

From equation A3, it follows that

$$b = T - (1/k_m)\, da/dt - a \qquad \textit{(Eq. A6)}$$

and by differentiation

$$-db/dt = da/dt + (1/k_m)\, d^2a/dt^2 \qquad \textit{(Eq. A7)}$$

By substituting equations A5, A6, and A7 into equation A1, we get

$$d^2a/dt^2 + (k_m + k_3(1 + B/E))\, da/dt + k_m\, k_3\, a = k_m\, k_3\, T \qquad \textit{(Eq. A8)}$$

with the solution

$$(1 - a/a_\infty) = C1\, e^{-\alpha t} + C2\, e^{-\beta t};\ (C1 + C2) = 1 \text{ [Eq. 6]} \qquad \textit{(Eq. A9)}$$

where in isotopic equilibrium ($t = \infty$), $T = a_\infty$ and $A >> (B + E)$. The integration constants C1 and C2 and the rate coefficients α and β are related to the theoretical constants k_3, k_m, and B/E by

$$k_m = \alpha + \beta - \alpha\beta/(\alpha\, C1 + \beta\, C2) \text{ [Eq. 7]} \qquad \textit{(Eq. A10)}$$

$$k_3 = \alpha\, \beta/k_m \text{ [Eq. 8]} \qquad \textit{(Eq. A11)}$$

$$1 + B/E = k_m/(\alpha\, C1 + \beta\, C2) \text{ [Eq. 9]} \qquad \textit{(Eq. A12)}$$

Equation 9 is obtained as follows. Differentiation of equation 6 gives

$$d(a/a_\infty)/dt \to (\alpha\, C1 + \beta\, C2) \text{ for } t \to 0 \qquad \textit{(Eq. A13)}$$

where $a_\infty = (b_0 + e_0)$ at time zero. Therefore,

$$da/dt \to (\alpha\, C1 + \beta\, C2)\ (b_0 + e_0) \text{ for } t \to 0 \qquad \textit{(Eq. A14)}$$

Furthermore, $da/dt \to k_m\, e_0$ for $t \to 0$ according to equation A2. Because $e_0/E = b_0/B$, we get equation 9.

This study was supported by grants from the Novo Nordisk Foundation and the Carlsberg Foundation. Aase Frederiksen provided skilful technical assistance, and Nicolas Fain revised the language. Both contributions are gratefully acknowledged.

REFERENCES

1. Schmid, H. H. O., P. C. Schmid, and E. V. Berdyshev. 2002. Cell signaling by endocannabinoids and their congeners: questions of selectivity and other challenges. *Chem. Phys. Lipids.* **121:** 111–134.
2. Hansen, H. S., B. Moesgaard, H. H. Hansen, and G. Petersen. 2000. *N*-Acylethanolamines and precursor phospholipids—relation to cell injury. *Chem. Phys. Lipids.* **108:** 135–150.
3. Devane, W. A., L. Hanus, A. Breuer, R. G. Pertwee, L. A. Stevenson, G. Griffin, D. Gibson, A. Mandelbaum, A. Etinger, and R. Mechoulam. 1992. Isolation and structure of a brain constituent that binds to the cannabinoid receptor. *Science.* **258:** 1946–1949.
4. Sugiura, T., T. Kodaka, S. Nakane, T. Miyashita, S. Kondo, Y. Suhara, H. Takayama, K. Waku, C. Seki, N. Baba, et al. 1999. Evidence that the cannabinoid CB1 receptor is a 2-arachidonoylglycerol receptor—structure-activity relationship of 2-arachidonoylglycerol, ether-linked analogues, and related compounds. *J. Biol. Chem.* **274:** 2794–2801.
5. Zoratti, C., D. Kipmen-Korgun, K. Osibow, R. Malli, and W. F. Graier. 2003. Anandamide initiates Ca^{2+} signaling *via* CB_2 receptor linked to phospholipase C in calf pulmonary endothelial cells. *Br. J. Pharmacol.* **140:** 1351–1362.
6. Zygmunt, P. M., J. Petersson, D. A. Andersson, H. H. Chuang, M. Sorgård, V. Di Marzo, D. Julius, and E. D. Högestätt. 1999. Vanilloid receptors on sensory nerves mediate the vasodilator action of anandamide. *Nature.* **400:** 452–457.
7. Premkumar, L. S., and G. P. Ahern. 2000. Induction of vanilloid receptor channel activity by protein kinase C. *Nature.* **408:** 985–990.
8. Maingret, F., A. J. Patel, M. Lazdunski, and E. Honoré. 2001. The endocannabinoid anandamide is a direct and selective blocker of the background K^+ channel TASK-1. *EMBO J.* **20:** 47–54.
9. Howlett, A. C., F. Barth, T. I. Bonner, G. Cabral, P. Casellas, W. A. Devane, C. C. Felder, M. Herkenham, K. Mackie, B. R. Martin, et al. 2002. International Union of Pharmacology. XXVII. Classification of cannabinoid receptors. *Pharmacol. Rev.* **54:** 161–202.
10. Schmid, P. C., P. V. Reddy, V. Natarajan, and H. H. O. Schmid. 1983. Metabolism of *N*-acylethanolamine phospholipids by a mammalian phosphodiesterase of the phospholipase D type. *J. Biol. Chem.* **258:** 9302–9306.
11. Petersen, G., and H. S. Hansen. 1999. *N*-Acylphosphatidylethanolamine-hydrolysing phospholipase D lacks the ability to transphosphatidylate. *FEBS Lett.* **455:** 41–44.
12. Okamoto, Y., J. Morishita, K. Tsuboi, T. Tonai, and N. Ueda. 2004. Molecular characterization of a phospholipase D generating anandamide and its congeners. *J. Biol. Chem.* **279:** 5298–5305.
13. Cravatt, B. F., D. K. Giang, S. P. Mayfield, D. L. Boger, R. A. Lerner, and N. B. Gilula. 1996. Molecular characterization of an enzyme that degrades neuromodulatory fatty-acid amides. *Nature.* **384:** 83–87.
14. Deutsch, D. G., N. Ueda, and S. Yamamoto. 2002. The fatty acid amide hydrolase (FAAH). *Prostaglandins Leukot. Essent. Fatty Acids.* **66:** 201–210.
15. Hillard, C. J., and A. Jarrahian. 2003. Cellular accumulation of anandamide: consensus and controversy. *Br. J. Pharmacol.* **140:** 802–808.
16. Liu, J., S. Bátkai, P. Pacher, J. Harvey-White, J. A. Wagner, B. F. Cravatt, B. Gao, and G. Kunos. 2003. Lipopolysaccharide induces anandamide synthesis in macrophages via CD14/MAPK/phosphoinositide 3-kinase/NF-kappaB independently of platelet-activating factor. *J. Biol. Chem.* **278:** 45034–45039.
17. Cravatt, B. F., K. Demarest, M. P. Patricelli, M. H. Bracey, D. K. Giang, B. R. Martin, and A. H. Lichtman. 2001. Supersensitivity to anandamide and enhanced endogenous cannabinoid signaling in mice lacking fatty acid amide hydrolase. *Proc. Natl. Acad. Sci. USA.* **98:** 9371–9376.
18. Deutsch, D. G., M. S. Goligorsky, P. C. Schmid, R. J. Krebsbach, H. H. O. Schmid, S. K. Das, S. K. Dey, G. Arreaza, C. Thorup, G. Stefano, et al. 1997. Production and physiological actions of anandamide in the vasculature of the rat kidney. *J. Clin. Invest.* **100:** 1538–1546.
19. Bojesen, I. N., and H. S. Hansen. 2003. Binding of anandamide to bovine serum albumin. *J. Lipid Res.* **44:** 1790–1794.
20. Giuffrida, A., F. Rodriguez de Fonseca, F. Nava, P. Loubet-Lescoulié, and D. Piomelli. 2000. Elevated circulating levels of anandamide after administration of the transport inhibitor, AM404. *Eur. J. Pharmacol.* **408:** 161–168.
21. Di Marzo, V., A. Fontana, H. Cadas, S. Schinelli, G. Cimino, J-C. Schwartz, and D. Piomelli. 1994. Formation and inactivation of endogenous cannabinoid anandamide in central neurons. *Nature.* **372:** 686–691.
22. Fowler, C. J., and S. O. P. Jacobsson. 2002. Cellular transport of anandamide, 2-arachidonoylglycerol and palmitoylethanolamide—targets for drug development? *Prostaglandins Leukot. Essent. Fatty Acids.* **66:** 193–200.
23. Fegley, D., S. Kathuria, R. Mercier, C. Li, A. Goutopoulos, A. Makriyannis, and D. Piomelli. 2004. Anandamide transport is independent of fatty-acid amide hydrolase activity and is blocked by the hydrolysis-resistant inhibitor AM1172. *Proc. Natl. Acad. Sci. USA.* **101:** 8756–8761.
24. Fowler, C. J., G. Tiger, A. Ligresti, M. L. López-Rodriguez, and V. Di Marzo. 2004. Selective inhibition of anandamide cellular uptake versus enzymatic hydrolysis—a difficult issue to handle. *Eur. J. Pharmacol.* **492:** 1–11.
25. Ligresti, A., E. Morera, M. Van der Stelt, K. Monory, B. Lutz, G. Ortar, and V. Di Marzo. 2004. Further evidence for the existence of a specific process for the membrane transport of anandamide. *Biochem. J.* **380:** 265–272.
26. Fasia, L., V. Karava, and A. Siafaka-Kapadai. 2003. Uptake and metabolism of [^{3}H]anandamide by rabbit platelets—lack of transporter? *Eur. J. Biochem.* **270:** 3498–3506.
27. Glaser, S. T., N. A. Abumrad, F. Fatade, M. Kaczocha, K. M. Studholme, and D. G. Deutsch. 2003. Evidence against the presence of an anandamide transporter. *Proc. Natl. Acad. Sci. USA.* **100:** 4269–4274.
28. Kalant, D., and K. Cianflone. 2004. Regulation of fatty acid transport. *Curr. Opin. Lipidol.* **15:** 309–314.
29. Hajri, T., and N. A. Abumrad. 2002. Fatty acid transport across membranes: relevance to nutrition and metabolic pathology. *Annu. Rev. Nutr.* **22:** 383–415.
30. Stahl, A., R. E. Gimeno, L. A. Tartaglia, and H. F. Lodish. 2001. Fatty acid transport proteins: a current view of a growing family. *Trends Endocrinol. Metab.* **12:** 266–273.
31. Hamilton, J. A., and F. Kamp. 1999. How are free fatty acids transported in membranes? Is it by proteins or by free diffusion through the lipids? *Diabetes.* **48:** 2255–2269.
32. Kleinfeld, A. M., S. Storms, and M. Watts. 1998. Transport of long-chain native fatty acids across human erythrocyte ghost membranes. *Biochemistry.* **37:** 8011–8019.
33. Bojesen, I. N., and E. Bojesen. 1998. Nature of the elements transporting long-chain fatty acids through the red cell membrane. *J. Membr. Biol.* **163:** 169–181.
34. Bojesen, I. N., and E. Bojesen. 1999. Sheep erythrocyte membrane binding and transfer of long-chain fatty acids. *J. Membr. Biol.* **171:** 141–149.
35. Bojesen, I. N. 2002. Studies of membrane transport mechanism of long-chain fatty acids in human erythrocytes. *Recent Research in Development of Membrane Biology.* **1:** 33–50.
36. Bojesen, I. N., and E. Bojesen. 1991. Palmitate binding to and efflux kinetics from human erythrocyte ghost. *Biochim. Biophys. Acta.* **1064:** 297–307.
37. Bojesen, I. N., and E. Bojesen. 1995. Arachidonic acid transfer across the human red cell membrane by a specific transport system. *Acta Physiol. Scand.* **154:** 253–267.
38. Bojesen, I. N., and E. Bojesen. 1996. Oleic acid binding and transport capacity of human red cell membrane. *Acta Physiol. Scand.* **156:** 501–516.
39. Simons, K., and W. L. C. Vaz. 2004. Model systems, lipid rafts, and cell membranes. *Annu. Rev. Biophys. Biomol. Struct.* **33:** 269–295.
40. Ortega-Gutiérrez, S., E. G. Hawkins, A. Viso, M. L. Lopez-Rodriguez, and B. F. Cravatt. 2004. Comparison of anandamide transport in FAAH wild-type and knock out neurons: evidence for contributions by both FAAH and CB1 receptor to anandamide uptake. *Biochemistry.* **43:** 8184–8190.
41. Schaap, F. G., G. J. van der Vusse, and J. F. C. Glatz. 2002. Evolution of the family of intracellular lipid binding proteins in vertebrates. *Mol. Cell. Biochem.* **239:** 69–77.
42. Hanada, K., K. Kumagai, S. Yasuda, Y. Miura, M. Kawano, M. Fukasawa, and M. Nishijima. 2003. Molecular machinery for nonvesicular trafficking of ceramide. *Nature.* **426:** 803–809.